GEOMETRY AND PROBABILITY IN THREE DIMENSIONS

LOUIS J. BILLERA, KENNETH S. BROWN, AND PERSI DIACONIS

Abstract. This paper explains some modern geometry and probability in the course of solving a random walk problem. Consider n planes through the origin in three dimensional Euclidean space. Assume, for simplicity, that they are in general position. They then divide space into $n(n-1)+2$ regions. We study a random walk on these regions. Suppose the walk is in region C. Pick a pair of the planes at random. These determine a line through the origin. Pick one of the two halves of the line with equal probability. The walk now moves to the region adjacent to the chosen half-line which is closest to C. We determine the long-term stationary distribution: All regions of i sides have stationary probability proportional to $i-2$. We further show that the walk is close to its stationary distribution after two steps.

1. Introduction

The geometry of hyperplane arrangements in Euclidean space is a rich subject which touches geometry [13], combinatorics [20], and operations research [21]. Probability was introduced into the subject by Bidigare, Hanlon, and Rockmore [2], who found a natural family of random walks associated to hyperplane arrangements. These walks were studied further by Brown and Diaconis [5]. One reason this development is exciting is that the walks admit a rather complete theory. Our purpose in the present paper is to introduce the reader to this circle of ideas by specializing to the 3-dimensional case (planes in $\mathbb{R}^3$). Here we are able to use tools from geometry to obtain a surprising formula for the stationary distribution of the walk.

1.1. **The geometric setup.** Consider a collection $\mathcal{A}$ of n planes through the origin in $\mathbb{R}^3$. We exclude the case where $\mathcal{A}$ is a pencil, *i.e.*, where $\mathcal{A}$ consists of n planes passing through a common line. In particular, we must have $n \geq 3$. It is useful to picture the arrangement $\mathcal{A}$ via the intersection of the planes with the unit sphere S^2. See Figure 1 for the case where $\mathcal{A}$ consists of the three coordinate planes. The

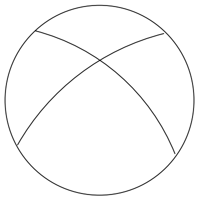

Figure 1. Three great circles on S^2.

picture shows the Northern Hemisphere, viewed from above the North Pole; thus

The first and third authors were supported in part by grants from the NSF.

the outer circle is the equator $z = 0$. Adding the plane $x + y + z = 0$ gives the picture in Figure 2.

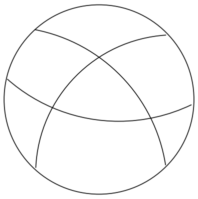

FIGURE 2. Four great circles on S^2.

The n great circles corresponding to the arrangement $\mathcal{A}$ decompose the sphere into cells: There are f_0 vertices, f_1 edges, and f_2 regions. When $n = 3$, for example, one has $f_0 = 6$, $f_1 = 12$, and $f_2 = 8$. Only the cells in the Northern Hemisphere are visible in the picture, but the Southern Hemisphere has exactly the same geometry. Notice that all the regions are triangular in Figure 1. In Figure 2 there are $f_2 = 14$ 2-dimensional cells: 8 triangles and 6 quadrilaterals, half of which are visible.

The cell decomposition induced by an arrangement has the following special property: *Given a region C and a vertex v, there is a unique region C' adjacent to v that is closest to C, in the sense that C' is separated from C by the minimum number of great circles.* The region C' is said to be the *projection* of C on v and is denoted vC. We will explain in Section 3.2 why it is uniquely defined. Figure 3 shows an example; here C' is at distance two from C.

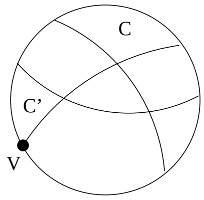

FIGURE 3. The projection of C on v.

1.2. **A random walk on the regions.** Bidigare, Hanlon, and Rockmore [2] used the projection operators to define the following walk on the regions: If the walk is in region C, choose a vertex v at random and move to the projection $C' = vC$. (We assume here that the vertices are chosen uniformly, so that all f_0 vertices are equally likely.) This walk is described mathematically by its *transition matrix* K. The rows and columns of K are indexed by the regions, with $K(C, C')$ being the chance of moving from C to C' in one step. Thus

$$K(C, C') = \frac{1}{f_0}\Lambda(C, C'),$$

where $\Lambda(C, C')$ is the number of vertices v of C' such that $vC = C'$.

Suppose, for instance, that $\mathcal{A}$ consists of the three coordinate planes. The 8 triangular regions are the intersections with the sphere of the 8 orthants in $\mathbb{R}^3$, as indicated in Figure 4. For example, the region $+-+$ corresponds to the orthant

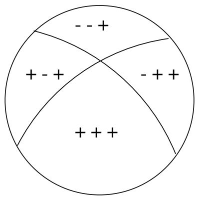

FIGURE 4. The regions correspond to orthants.

$x > 0$, $y < 0$, $z > 0$. The matrix Λ is shown below; one has $K = \frac{1}{6}\Lambda$.

	$+++$	$++-$	$+-+$	$+--$	$-++$	$-+-$	$--+$	$---$
$+++$	3	1	1	0	1	0	0	0
$++-$	1	3	0	1	0	1	0	0
$+-+$	1	0	3	1	0	0	1	0
$+--$	0	1	1	3	0	0	0	1
$-++$	1	0	0	0	3	1	1	0
$-+-$	0	1	0	0	1	3	0	1
$--+$	0	0	1	0	1	0	3	1
$---$	0	0	0	1	0	1	1	3

Notice that for any region C, the three vertices of C satisfy $vC = C$; this explains the diagonal entries of Λ. Projection onto each of the remaining three vertices flips C to an adjacent region, thus accounting for the three 1's in each row. At each step, then, the walk stays in its current region with probability $1/2$ and otherwise moves to a randomly chosen adjacent region. This example is unusual, in that one never moves a distance of more than 1 in any step; typically the walk is much more vigorous.

The ℓ^{th} power of the matrix K gives the transition probabilities after ℓ steps; for example,

$$K^2(C, C') = \sum_{C''} K(C, C'')K(C'', C'),$$

which is the chance of moving from C to C' in two steps. After all, to get from C to C' in two steps the walk must go to some C'' and then to C'.

A fundamental theorem of Markov chain theory [16] implies that $K^\ell(C, C')$ tends to a limit $\pi(C')$, independent of the starting region C:

$$K^\ell(C, C') \to \pi(C') \quad \text{as } \ell \to \infty.$$

Here π is a probability distribution on the set of regions, and $\pi(C')$ represents the chance that the random walk is in C' after a large number of steps from any starting region C. The distribution π is called the *stationary distribution* of the walk. It can be characterized as the unique probability distribution satisfying

$$\sum_{C} \pi(C)K(C, C') = \pi(C') \tag{1}$$

for all C'. This says that π, viewed as a row vector, is a left eigenvector for K with eigenvalue 1.

1.3. **Analysis of the walk.** Bidigare, Hanlon, and Rockmore [2] determined the eigenvalues of K, which turn out to be real (and even rational):

(a) 1 is an eigenvalue of multiplicity 1.
(b) For each plane $H \in \mathcal{A}$, there is an eigenvalue

$$\lambda_H = \frac{\#\text{ of vertices on } H \cap S^2}{f_0}$$

of multiplicity 1.
(c) $2/f_0$ is an eigenvalue of multiplicity $(f_2 - 2)/2$.
(d) 0 is an eigenvalue of multiplicity $(f_2 - 2)/2 - n + 1$.

A different proof of this can be found in [5], where it is shown further that K is diagonalizable. For a simple example, take $n = 3$ again; the 8 eigenvalues are then $1, \frac{2}{3}, \frac{2}{3}, \frac{2}{3}, \frac{1}{3}, \frac{1}{3}, \frac{1}{3}, 0$.

A second result of [2, 5] is a surprisingly simple estimate relating the eigenvalues to the rate of convergence to stationarity. Let K_C^ℓ be the distribution of the walk started from C after ℓ steps, *i.e.*, $K_C^\ell(C') = K^\ell(C, C')$. We measure distance to stationarity by means of the *total variation distance* $\|K_C^\ell - \pi\|$, defined as follows: If P and Q are probability distributions on a finite set X, then

$$\|P - Q\| = \max_{A \subseteq X} |P(A) - Q(A)| \tag{2}$$

The version of the convergence rate estimate given in [5] is

$$\|K_C^\ell - \pi\| \le \sum_{H \in \mathcal{A}} \lambda_H^\ell, \tag{3}$$

for any starting region C. When $n = 3$, for example, the distance to stationarity is bounded by $3\left(\frac{2}{3}\right)^\ell$ after ℓ steps.

Finally, a method is given in [5] for computing the stationary distribution π, though it is not always easy to get a useful formula for π by this method. The new result of the present paper is that there is in fact such a formula in the 3-dimensional case:

Theorem 1 (Main theorem). *Let $\mathcal{A}$ be an arrangement of n planes through the origin in $\mathbb{R}^3$, and assume that $\mathcal{A}$ is not a pencil. Let π be the stationary distribution of the random walk on regions of the sphere, as described above. If C is a region with i sides, then*

$$\pi(C) = \frac{i - 2}{2(f_0 - 2)}.$$

We find this result quite surprising. It is not even obvious to us why all i-gons should have the same stationary probability, let alone why this probability should be proportional to $i-2$. In our $n = 3$ example, the theorem says that the stationary distribution is uniform: $\pi(C) = \frac{1}{8}$ for each of the 8 triangles C.

1.4. **Organization of the paper.** In Section 2 we will make a number of remarks about the main theorem and illustrate it with examples. Section 3 gives some background on hyperplane arrangements in order to put the results stated above into a broader context. We also state in Section 3 some of the results of [2, 5] which were specialized to the 3-dimensional case above. In Section 4 we show how the general theory specializes to card shuffling and random tiling models. In Section 5 we give a geometric description of the matrix K in the 3-dimensional case. With this description available, it is quite easy to verify the main theorem; we do this in Section 6. Finally, Section 7 contains some pointers to the literature on plane arrangements in $\mathbb{R}^3$.

The key arguments of this paper represent the combinatorial essence of a hyperplane arrangement as a collection of sequences of signs; see Section 3. This can be abstracted to the notion of an oriented matroid. The present project makes a nice introduction to these ideas.

Acknowledgments. We thank Catherine Stenson and Eli Goodman for helpful comments.

2. Examples and remarks

We continue to denote by $\mathcal{A}$ an arrangement of n planes in $\mathbb{R}^3$, which is not a pencil.

2.1. **General position.** The n planes are said to be in *general position* if no three of the planes have a nonzero intersection or, equivalently, if only two great circles pass through each vertex on the sphere. Many of the examples in this paper are in fact in general position; but the simplicial arrangements to be discussed in Section 2.3 are never in general position unless $n = 3$, nor are the arrangements in Section 4 below.

It is easy to count cells in the general position case. One finds

$$\begin{aligned} f_0 &= n(n-1) \\ f_1 &= 2n(n-1) \\ f_2 &= n(n-1) + 2. \end{aligned}$$

In fact, there are $\binom{n}{2}$ pairs of great circles, each determining a pair of antipodal vertices, whence the first equation. For the second equation, note that each of the n great circles is cut into $2(n-1)$ arcs by the other $n-1$ great circles. [Alternatively, count the vertex-edge pairs in two different ways to get $2f_1 = 4f_0$, so that $f_1 = 2f_0$.] Finally, the third equation can be proved by a straightforward inductive argument, or it can be deduced from the first two via Euler's relation $f_0 - f_1 + f_2 = 2$.

The list of eigenvalues λ and multiplicities m_λ given in Section 1.3 becomes

λ	m_λ
1	1
$2/n$	n
$1/\binom{n}{2}$	$\binom{n}{2}$
0	$\binom{n}{2} - n + 1$

And the convergence rate estimate (3) is

$$\|K_C^\ell - \pi\| \le n \left(\frac{2}{n}\right)^\ell .$$

This shows that the distance to the stationary distribution is small after $\ell = 2$ steps if n is large. In Section 5.3, after we have a geometric description of the transition matrix K, we will be able to give examples of families of arrangements of n hyperplanes such that $\|K_C - \pi\| \ge c > 0$ for all n. In this sense the walk is close to stationary after 2 steps but not after 1.

Another feature of the general position case is that if one wants to carry out the random walk algorithmically, it is quite easy to pick a random vertex: First pick a pair of great circles at random, so that all $\binom{n}{2}$ are equally likely; this defines a pair of antipodal points. Now choose one of these two points with probability $\frac{1}{2}$.

Finally, Theorem 1 gives the following formula for the stationary distribution π in the general position case:

$$\pi(C) = \frac{i-2}{2(n(n-1)-2)}$$

if C is an i-gon.

Here are some specific examples:

Example 1. For $n = 3$, the arrangement is combinatorially equivalent to that of Figure 1. There are 8 triangular regions, and the stationary distribution is $\pi(C) = \frac{1}{8}$ for all C.

Example 2. For $n = 4$ planes in general position (Figure 2) there are 14 regions: 8 triangles with stationary probability $\pi(C) = \frac{1}{20}$ and 6 quadrilaterals with $\pi(C) = \frac{2}{20}$.

Example 3. With $n = 5$ planes in general position, the situation is as in Figure 5 up to isomorphism. There are 10 triangles with $\pi(C) = \frac{1}{36}$, 10 quadrilaterals with $\pi(C) = \frac{2}{36}$, and 2 pentagons with $\pi(C) = \frac{3}{36}$.

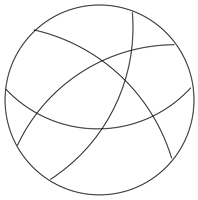

FIGURE 5. Five great circles in general position.

Example 4. With $n = 6$ or more planes the number of regions of each type can vary with the actual arrangement. From the catalogue in Grünbaum [11, 13] one sees that up to combinatorial equivalence there are exactly four general position arrangements of 6 planes, as shown in Figure 6. The number of i-gons ($i = 3, 4, 5, 6$)

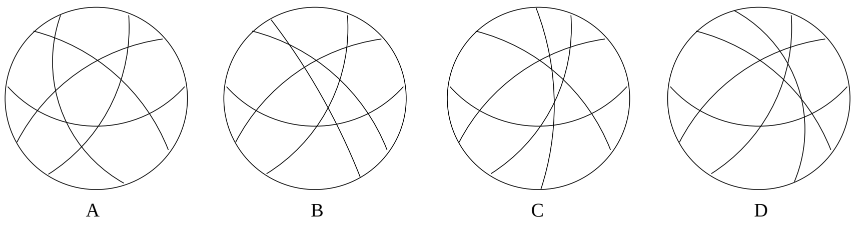

FIGURE 6. Six great circles in general position.

for each of these four arrangements is shown in Table 1. Each arrangement has

$n(n-1)+2 = 32$ regions. For each arrangement, the stationary probability of an i-gon is $\frac{i-2}{56}$. Note that, for some values of i, some arrangements don't have any i-gons. Nonetheless, the stationary probabilities sum to 1.

i	A	B	C	D
3	20	14	12	12
4	0	12	16	18
5	12	6	4	0
6	0	0	0	2

TABLE 1. The number of i-gons.

2.2. **The Euler relation.** For a given arrangement of n planes, let p_i be the number of i-sided regions. Since the stationary probabilities in Theorem 1 must sum to 1, we get

$$\sum_{i=3}^{n} p_i \frac{(i-2)}{2(f_0-2)} = 1. \tag{4}$$

We now show that this relation is equivalent to the Euler relation $f_0 - f_1 + f_2 = 2$. Rewrite (4) as $\sum ip_i - 2\sum p_i = 2(f_0-2)$. The first sum is the number of pairs consisting of a region and an edge of that region; since each edge is on exactly two regions, this sum equals $2f_1$. The second sum is f_2. So (4) becomes $2f_1 - 2f_2 = 2(f_0-2)$, which is Euler's identity.

2.3. **Simplicial arrangements.** The arrangement $\mathcal{A}$ is said to be *simplicial* if every region on the sphere is a triangle. The simplicial case has long held a special fascination for geometers (cf. [12, 13]). And it is of special interest for the probability story also. In fact, every arrangement has some triangles (at least n of them by Levi's theorem, cf. [13, p. 25]); so Theorem 1 has the following consequence:

Proposition 1. *The random walk on regions has a uniform stationary distribution if and only if the arrangement is simplicial.*

There are three known infinite families of simplicial arrangements and 90 "sporadic" examples. It has been conjectured that there are no more infinite families and at most finitely many additional sporadic examples; see [13, p 8, Conjecture 2.1]. A catalogue showing the first 89 sporadic examples can be found in [12], and the 90th is in [13]. [Note: It is stated in [13] that there are 91 sporadic examples, but the arrangements called $A_2(17)$ and $A_7(17)$ in [12] have been shown to be isomorphic; see [14, p. 59].] Many of the examples have a great deal of symmetry, and one is therefore not surprised when the stationary distribution turns out to be uniform. But there is one known example ([13, pp. 8–9]) of a simplicial arrangement whose group of combinatorial symmetries is trivial. Nevertheless, the walk on the regions has a uniform stationary distribution. This example, which has $n = 28$, is shown in Figure 7 in its projective representation. We will discuss such representations in Section 7; for now, suffice it to say that we get the spherical representation by drawing the lines in Figure 7 as great semicircles on the Northern Hemisphere. Parallel lines yield great semicircles with the same endpoints on the equator.

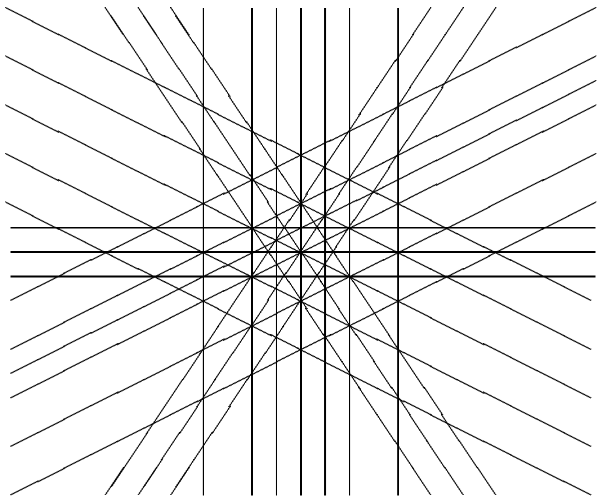

FIGURE 7. A simplicial arrangement with no symmetry (projective picture); the line at infinity is included.

2.4. **Arrangements of pseudocircles.** The theory developed in [5] and in the present paper goes through if the family of great circles is replaced by a family of "pseudocircles", *i.e.*, simple closed curves on the sphere that are not necessarily great circles but merely intersect as great circles would. See [4, 13, 21] for the precise definition and many examples. The reason the theory goes through is that, as we remarked in the introduction, all of our work is based on the oriented matroid underlying the arrangement, and this exists for arrangements of pseudocircles also. Generalizing in this way is of interest because it vastly increases the supply of examples. In particular, one obtains seven new infinite families of simplicial arrangements. See [13, 10].

3. Hyperplane arrangements

A good reference for the theory of hyperplane arrangements is the book by Orlik and Terao [19]. See also [18, 4, 21] and, for a concise summary of the basic concepts, [5, §2]. This section and the next are included mostly to provide some context for the seemingly strange random walk introduced in Section 1. Except for the sign sequences discussed below, the results stated in these two sections will not be used in the remainder of the paper.

Throughout this section $\mathcal{A} = \{H_i\}_{i \in I}$ will denote a finite set of linear hyperplanes (subspaces of codimension 1) in a finite dimensional real vector space V. One often assumes that $\mathcal{A}$ is *essential*, meaning that the intersection of the hyperplanes is the trivial subspace. When $V = \mathbb{R}^3$, this is the same as saying that $\mathcal{A}$ is not a pencil. There is no loss of generality in restricting to essential arrangements. Indeed, an inessential arrangement can be viewed as an essential arrangement in the quotient space V/V_0, where $V_0 = \bigcap_{i \in I} H_i$.

3.1. **Chambers.** The open regions into which V is cut by $\mathcal{A}$ are called *chambers*. More precisely, the chambers are the connected components of the complement of $\bigcup_{i \in I} H_i$ in V. We denote by $\mathcal{C}$ the set of chambers. For example, if $\mathcal{A}$ consists of the

d coordinate hyperplanes $x_i = 0$ in $\mathbb{R}^d$ ($i = 1, \dots, d$), then there are 2^d chambers (the orthants). In this example a chamber C can be encoded by a *sign sequence* $\sigma_1, \dots, \sigma_d$, where σ_i gives the sign of the i^{th} coordinate x_i for points in C; here σ_i is one of the symbols $+, -$. For $d = 3$ this was illustrated in Section 1 (Figure 4).

There is a similar sign encoding of the chambers for an arbitrary $\mathcal{A}$: For each $H \in \mathcal{A}$ let H^+ and H^- be the two open halfspaces in V determined by H. (The choice of which one to call H^+ is arbitrary but fixed.) Then the chambers are precisely the nonempty sets of the form

$$C = \bigcap_{i \in I} H_i^{\sigma_i},$$

where $\sigma_i = \pm$. The vector of signs $(\sigma_i)_{i \in I}$ provides a succinct description of C. Figure 8 illustrates this for the four planes $x = 0$, $y = 0$, $z = 0$, $x + y + z = 0$. Here, as in Section 1, we use the spherical representation of the arrangement, so that the planes correspond to great circles and the chambers correspond to regions on the sphere. The region labeled $++++$, for instance, corresponds to the chamber $x > 0$, $y > 0$, $z > 0$, $x + y + z > 0$. The fourth inequality is redundant, so the chamber only has three bounding planes and its intersection with the sphere is a triangle. Notice that the sign vectors of the remaining chambers can be filled in once $++++$ has been identified; just move from chamber to chamber, crossing one plane at a time and recording the appropriate sign change.

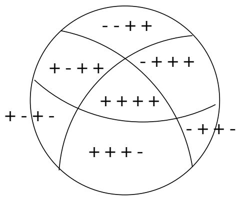

FIGURE 8. Sign vectors for four planes in general position.

3.2. **Faces and projections.** The chambers are defined by finitely many (strict) linear inequalities, hence they are polyhedra. They therefore have *faces*, which are the nonempty sets obtained by changing zero or more inequalities to equalities. (More precisely, these are the *relatively open faces*.) Let $\mathcal{F}$ be the set of all faces of all chambers. Then $\mathcal{F}$ consists of all nonempty sets of the form

$$F = \bigcap_{i \in I} H^{\sigma_i},$$

where now $\sigma_i \in \{+, -, 0\}$ and $H_i^0 = H_i$. Thus faces, like chambers, are encoded by sign sequences. In the example above, the chamber $++++$ has three faces of codimension 1, with sign sequences $0{+}{+}{+}$, ${+}0{+}{+}$, and ${+}{+}0{+}$. These correspond to the three sides of the triangle labeled $++++$ in Figure 8. Note that ${+}{+}{+}0$ does not occur, because it would correspond to the inconsistent set of inequalities $x > 0$, $y > 0$, $z > 0$, $x + y + z = 0$.

Remark. The faces are in 1–1 correspondence with their intersections with the unit sphere. If the arrangement $\mathcal{A}$ is essential, these intersections give a cell-decomposition of the sphere, as we have already seen in the case $V = \mathbb{R}^3$.

There is a natural poset structure on the set of faces: Given $F, G \in \mathcal{F}$, we write $F \leq G$ and say that F is a *face* of G if the sign vector of F is obtained from that of G by changing zero or more components to 0. Less obviously, $\mathcal{F}$ admits a *semigroup structure*: Given $F, G \in \mathcal{F}$ with sign vectors $\sigma(F), \sigma(G)$, their product FG is the cell with sign vector

$$\sigma_i(FG) = \begin{cases} \sigma_i(F) & \text{if } \sigma_i(F) \neq 0 \\ \sigma_i(G) & \text{if } \sigma_i(F) = 0. \end{cases}$$

This has a geometric interpretation: If we move on a straight line from a point of F toward a point of G, then FG is the face we are in after moving a small positive distance.

Given $F \in \mathcal{F}$ and $C \in \mathcal{C}$, their product FC is again a chamber, called the *projection* of C on F. It can be characterized as the nearest chamber to C having F as a face. Here "nearest" refers to the number of hyperplanes in $\mathcal{A}$ separating C from FC. This proves the existence of the projection operators which were used to construct the random walk in Section 1. We will see in Section 3.4 that a similar walk exists for an arbitrary hyperplane arrangement. First, we give an illustration of the use of sign vectors.

3.3. **The diameter of the walk in $\mathbb{R}^3$.** Consider an arrangement in $\mathbb{R}^3$ and the walk on regions defined in Section 1. The *diameter* of the walk is the smallest ℓ so that $K^{\ell}(C, C') > 0$ for all C, C'. In other words, it is the smallest ℓ so that one can get from any region to any other in ℓ steps. As an example, consider the arrangement of three planes shown (in its spherical representation) in Figure 1. By inspection, to get from a chamber to its antipode by steps of the walk (through a choice of vertices) takes three steps, and this is in fact the diameter.

Proposition 2. *The diameter of the walk based on n planes in $\mathbb{R}^3$ is always either 2 or 3. It is 2 if $n \geq 5$ and the planes are in general position.*

Proof. One can never get from a region C to its antipode $-C$ in one step; in fact, each vertex v has at least two 0's in its sign vector, so multiplying by v cannot change all the signs of C. This shows that the diameter is at least two.

Consider two regions C, C', with C' an m-gon. Assume, to simplify notation, that the sign vector σ' of C' has $\sigma'_j = +$ for all j and that the first m components correspond to the m sides of C'. Then C' is the unique region whose sign vector has $+$ in its first m positions. If $m \geq 4$, we can find vertices v, w of C' such that v is on two of the sides of C' and w is on two different sides. Thus the sign vector of v has 0 in two of the first m slots and $+$ in the rest, and similarly for w, with the 0's of v and w in disjoint positions. The product vwC in the semigroup $\mathcal{F}$ therefore has $+$ in its first m positions, *i.e.*, $vwC = C'$, and we can get from C to C' in two steps. This does not work if C' is a triangle ($m = 3$), but in that case we can get from any C to C' by using all three of the vertices of C'. Thus we have proved that the diameter is at most 3.

Finally, suppose that the planes are in general position, that $m = 3$, and that $n \geq 5$. Let w be a vertex on two of the great circles other than the three forming the sides of C'. In view of general position, the first 3 components of the sign vector of w are nonzero. Replacing w by $-w$ if necessary, we may assume that two of these 3 components, say the first two, are $+$. Let v be the vertex of C' whose sign vector has 0 in the first two slots. Then vw has $+$ everywhere, so we can get from C to C' in two steps. $\square$

3.4. **A walk on the chambers.** Returning to a general hyperplane arrangement, we may specify a random walk on $\mathcal{C}$ by assigning a weight w_F to each $F \in \mathcal{F}$. These weights satisfy $w_F \geq 0$ (many may be zero) and $\sum_{F\in\mathcal{F}} w_F = 1$. Given a starting chamber C_0, the walk proceeds by choosing from $\mathcal{F}$ with replacement, with w_F the chance of picking F each time. This generates choices $F_1, F_2, F_3, \ldots$. The walk proceeds by multiplying by F_i at stage i, *i.e.*, by projecting onto F_i. Thus it goes

$$C_0,\ F_1C_0,\ F_2F_1C_0, \ldots, F_iF_{i-1}\cdots F_1C_0, \ldots.$$

The chance of moving from C to C' in one step is

$$K(C, C') = \sum_{FC=C'} w_F. \tag{5}$$

The walk of Section 1 is based on n planes in $\mathbb{R}^3$ with $w_F = 0$ unless F is a half line (so that its intersection with the sphere is a point) and $w_F = 1/f_0$ for all half lines.

3.5. **Analysis of the walk.** As we remarked in the introduction, the hyperplane walks admit a rather complete theory. Bidigare–Hanlon–Rockmore [2] gave all the eigenvalues of the matrix K in a simple closed form. (We stated a special case of their result in Section 1.) The matrix was shown to be diagonalizable in [5]. The paper [5] also contains a description of the stationary distribution and a bound on the convergence rate. These results are stated in Theorem 2 below.

Call the system of weights $\{w_F\}_{F\in\mathcal{F}}$ *separating* if the weights are not concentrated on faces all contained in a single hyperplane. In symbols, for each $H \in \mathcal{A}$ there is $F \not\subseteq H$ with $w_F > 0$. As an example, the walk in Section 1 is separating since the vertices are obviously not all on one great circle.

Theorem 2 (Brown–Diaconis [5])**.** *Let $\mathcal{A}$ be a hyperplane arrangement. Let $\{w_F\}$ be a probability distribution on the set $\mathcal{F}$ of faces. Let $K(C, C')$ be defined by (5). Then*

(a) *K has a unique stationary distribution π if and only if $\{w_F\}$ is separating.*
(b) *If $\{w_F\}$ is separating, π may be described as follows: Sample* without *replacement from $\mathcal{F}$ according to the weights w_F. This generates an ordering $F_1, F_2, \ldots, F_m$ of $\{\, F \in \mathcal{F} : w_F > 0 \,\}$. The product $F_1F_2\cdots F_mC_0$ is independent of C_0 and is a chamber distributed according to π.*
(c) *If $\{w_F\}$ is separating, then for any $C_0 \in \mathcal{C}$ and positive integer ℓ*

$$\|K^{\ell}_{C_0} - \pi\| \leq \sum_{H\in A} \lambda_H^{\ell}, \quad \textit{where } \lambda_H = \sum_{F\subseteq H} w_F.$$

Part (c) of Theorem 2 immediately gives the convergence rate bound stated in Section 1. And part (b) of Theorem 2 can be used to get the explicit formula for π in the 3-dimensional case, as stated in Theorem 1. Indeed, we first discovered the formula by doing exactly that. It turns out, however, that one can give an easier and completely self-contained proof of Theorem 1 by a direct argument based on equation (1). That is what we will do in Section 6.

4. Two examples

There are many hyperplane arrangements where the chambers can be labeled in a natural way by familiar combinatorial objects such as permutations or trees and the walk above captures a natural mixing process. In this section we describe two such examples. The first is the braid arrangement, for which the chambers correspond to permutations. The action of faces on chambers gives natural shuffling schemes, such as the usual method of riffle shuffling a deck of cards, or a list rearrangement scheme used in computer science where a card is removed and replaced on top. The second example shows how hyperplane arrangements are related to tilings. In particular, we describe in some detail a hyperplane arrangement in $\mathbb{R}^3$ whose chambers correspond to rhombic tilings of a 10-gon. See [2, 5] for further examples.

4.1. **The braid arrangement and card shuffling.** The *braid arrangement* in $\mathbb{R}^d$ consists of the $\binom{d}{2}$ hyperplanes $H_{ij} = \{ (x_1, \ldots, x_d) : x_i = x_j \}$ $(i < j)$. The chambers are associated to a common ordering of the coordinates and so to one of the $d!$ permutations. When $d = 4$, for example, one of the 24 chambers is the region defined by $x_1 > x_4 > x_2 > x_3$, corresponding to the permutation 1423.

The braid arrangement is not essential, because the H_{ij} intersect in the line $x_1 = \cdots = x_d$. It therefore gives rise to an essential arrangement in a $(d-1)$-dimensional space, as explained at the beginning of Section 3. When $d = 4$, the resulting arrangement of 6 planes in $\mathbb{R}^3$ may be pictured as in Figure 9. The great circle corresponding to H_{ij} is labeled *i-j*. (The equator is *not* one of the great circles of the arrangement.) Each chamber is labeled with the associated permutation.

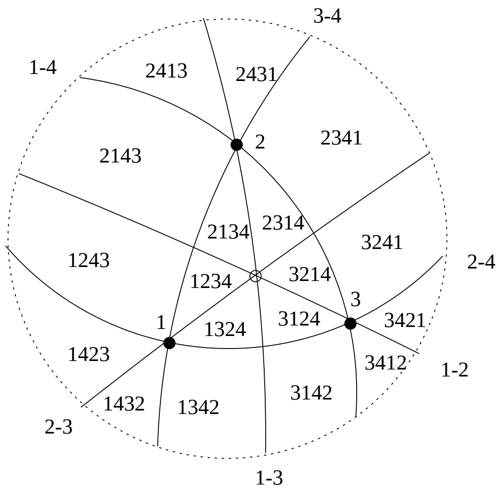

Figure 9. The braid arrangement when $d = 4$.

The faces of a chamber C are obtained by changing some of the inequalities defining C to equalities. For example, the chamber $x_2 > x_3 > x_1 > x_4$ has a face given by $x_2 > x_3 > x_1 = x_4$, which is also a face of the chamber $x_2 > x_3 > x_4 > x_1$. This common face is represented by the edge between 2314 and 2341 in Figure 9. Similarly, the vertex labeled 2 in the figure corresponds to the face $x_2 > x_1 = x_3 = x_4$; it is a face of six chambers, corresponding to the six possible orderings of the indices 1,3,4.

It is useful to encode the system of equalities and inequalities defining a face F by an *ordered partition* $(B_1, \ldots, B_k)$ of $\{1, \ldots, d\}$. Here $B_1, \ldots, B_k$ are disjoint nonempty sets whose union is $\{1, \ldots, d\}$; they are called the *blocks* of the partition, and their order counts. For example, the face $x_2 > x_3 > x_1 = x_4$ discussed above corresponds to the 3-block ordered partition $(\{2\}, \{3\}, \{1, 4\})$, and the face $x_2 > x_1 = x_3 = x_4$ [vertex 2 in the picture] corresponds to the 2-block ordered partition $(\{2\}, \{1, 3, 4\})$. Notice that there is also a (unique) 1-block ordered partition, corresponding to the face $x_1 = x_2 = x_3 = x_4$. When we pass from $\mathbb{R}^4$ to a 3-dimensional quotient to make the arrangement essential, this face becomes $\{0\}$. It does not show up in Figure 9 because its intersection with the sphere is empty.

The action of faces on chambers is easily pictured by thinking of a permutation $\tau = (\tau_1, \ldots, \tau_d)$ as the set of labels on a deck of d cards, with the card labeled τ_1 on top, and so on. The ordered partition $B = (B_1, B_2, \ldots)$ operates on τ by removing cards with labels in B_1 and placing them on top (keeping them in the same relative order), then removing cards with labels in B_2 and placing them next, and so on. Suppose, for example, that $d = 10$, $\tau = (1, 7, 3, 9, 10, 4, 5, 2, 6, 8)$, and $B = (\{2, 5\}, \{3, 4, 6, 10\}, \{7\}, \{1, 8, 9\})$; then B acting on τ gives $(5, 2, 3, 10, 4, 6, 7, 1, 9, 8)$.

The walk on chambers described in Section 3 now yields a variety of shuffling schemes, depending on the choice of weights w_F. One example that has received much attention is the "Tsetlin library", or "random-to-top" shuffle. Here one assigns a positive weight w_i to each 2-block ordered partition $(\{i\}, \{1, \ldots, d\} \setminus \{i\})$, and weight 0 to the other faces. When $d = 4$, for example, the vertices with positive weight are those labeled 1,2,3 in Figure 9 and the one that would be labeled 4 if it were visible. [The opposite vertex is shown as an open circle.] In the resulting random walk, a card is repeatedly picked at random according to the weights w_i and replaced on top. This walk is useful in connection with self-organizing list-management schemes [8]. Imagine, for instance, a stack of d files, where file i is used with frequency w_i. Each time a file is used, it is replaced on top of the stack. After the process has been running for a long time, the most frequently used files will tend to be near the top.

The basic walk studied in this paper, where the vertices are weighted uniformly, is itself quite interesting when applied to the braid arrangement. Here, we assign weight $1/(2^d - 2)$ to each of the $2^d - 2$ two-block ordered partitions. The corresponding shuffling mechanism consists of "inverse riffle shuffles". In an ordinary riffle shuffle a deck of cards is divided into two piles which are riffled together. The inverse chooses a set S of cards which are removed ("unriffled") and placed on top; the $2^d - 2$ proper nonempty subsets S are all equally likely to be unriffled. This is very closely related to a standard model for riffle shuffling. See [2, 5] for further details and references to earlier work.

To conclude, let us apply the results of Section 1.3 to the walk when $d = 4$ and the vertices are chosen uniformly. There are 14 vertices, 36 edges, and 24 regions. The stationary distribution is uniform because each of the regions has three sides. The eigenvalues and multiplicities (λ, m_λ) are $(1, 1)$, $(\frac{3}{7}, 6)$, $(\frac{1}{7}, 11)$, and $(0, 6)$. After shuffling ℓ times, the distance to stationarity satisfies

$$\|K^\ell - \pi\| \leq 6 \left(\frac{3}{7}\right)^\ell .$$

This bound shows that $\ell = 5$ shuffles suffice to make the distance to stationarity smaller than $1/10$.

4.2. **Arrangements and tilings.** We discuss now an example of an arrangement in $\mathbb{R}^3$ in which the chambers correspond to certain tilings of a centrally symmetric 10-gon. The walks described in this paper can then be used to generate random tilings. Such tilings are of interest to physicists who study quasicrystals (see [7, 15] and the references cited there). This is an example of a very general theory whereby hyperplane arrangements can be associated with a set of tilings of special convex polytopes called zonotopes [3, §4]. A good introductory reference for the material in this subsection is [21, Lecture 7].

Given n pairwise linearly independent vectors $v_1, \dots, v_n \in \mathbb{R}^d$, we define a convex polytope known as a *zonotope* by

$$Z(v_1, \dots, v_n) := \left\{ \sum_i \lambda_i v_i \mid 0 \le \lambda_i \le 1 \right\}.$$

We call the v_i the *zones* of $Z(v_1, \dots, v_n)$. When $d = 2$, $Z(v_1, \dots, v_n)$ is a centrally symmetric $2n$-gon; this is illustrated in Figure 10 for the case $d = 2$ and $n = 5$, where the resulting zonotope is a 10-gon.

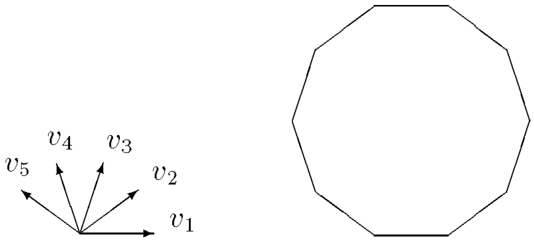

FIGURE 10. Five vectors in $\mathbb{R}^2$ and the 10-gon they generate.

We are interested in tilings of this 10-gon by the parallelograms generated by the $\binom{5}{2} = 10$ pairs v_i, v_j, $1 \le i < j \le 5$. Since we may take all the v_i to have the same length without loss of generality, we call these tilings *rhombic* tilings. Two such rhombic tilings are illustrated in Figure 11. It is a consequence of the theory

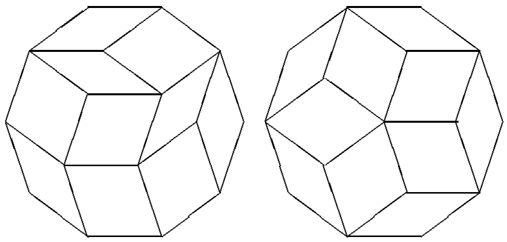

FIGURE 11. Two tilings of the 10-gon by parallelograms.

of *fiber polytopes* [3] that the set of all such tilings of this 10-gon corresponds to the chambers of an arrangement of $\binom{5}{3} = 10$ hyperplanes in $\mathbb{R}^3$, known as the *fiber arrangement* of the 10-gon. We describe this arrangement in some detail now.

Every triple of points v_i, v_j, v_k, $i < j < k$, satisfies a unique (up to nonzero scalar) linear dependence relation. Let $\tau = \{i, j, k\}$ and let the dependence be given by $z^\tau \in \mathbb{R}^5$; thus $\sum_{\ell=1}^5 z_\ell^\tau v_\ell = 0$ and $z_\ell^\tau = 0$ if $\ell \notin \tau$. The span V of the z^τ, over all triples $\tau \subset \{1,2,3,4,5\}$, is the nullspace of the rank 2 matrix

$$A = \begin{pmatrix} x_1 & x_2 & x_3 & x_4 & x_5 \\ y_1 & y_2 & y_3 & y_4 & y_5 \end{pmatrix},$$

where $v_i = (x_i, y_i)$, and so is 3-dimensional. For each triple τ, we denote by $H^\tau \subset \mathbb{R}^5$ the hyperplane having z^τ as its normal (*i.e.*, $H^\tau = \{x \in \mathbb{R}^5 \mid \langle x, z^\tau \rangle = 0\}$). The arrangement $\{H^\tau\}$ is not essential; in fact, $\cap_\tau H^\tau$ is the 2-dimensional space $V^\perp$ (the row space of A). We therefore get an essential arrangement in the 3-dimensional space $\mathbb{R}^5/V^\perp$ (which we may identify with V), as explained at the beginning of Section 3. This may be pictured as in Figure 12. Each great circle is

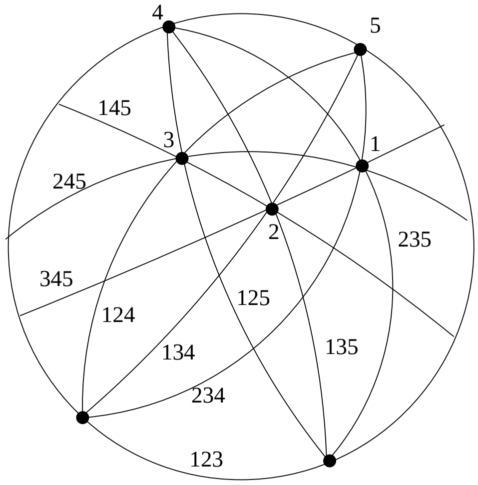

FIGURE 12. The fiber arrangement of a 10-gon.

labeled by the corresponding triple τ. Note that the 4 great circles corresponding to triples $\tau \subset \{2,3,4,5\}$ intersect at a pair of antipodal vertices, one of which is labeled 1 in the figure. This can be explained by straightforward linear algebra, which we leave to the interested reader. [Hint: Consider the matrix obtained from A by deleting the first column.] The other multiple intersections (with labels $2,\ldots,5$) can be explained in a similar way.

We claim that the chambers of this arrangement correspond to the rhombic tilings of the 10-gon. To understand why this might be so, take any point $\theta = (\theta_1,\ldots,\theta_5) \in \mathbb{R}^5$ not on any of the hyperplanes H^τ. Define the *lifted zones* $\widetilde{v}_i = (x_i, y_i, \theta_i)$, $i = 1,\ldots,5$, and the 3-dimensional *lifted zonotope* $\widetilde{Z} := Z(\widetilde{v}_1,\ldots,\widetilde{v}_5) \subset \mathbb{R}^3$. One can show that each 2-dimensional face of $\widetilde{Z}$ is a parallelogram.[1] Projecting the faces on the *bottom* of $\widetilde{Z}$ (*i.e.*, the faces whose outer normal has a negative third coordinate) onto the 10-gon $Z(v_1,\ldots,v_5)$, one gets a rhombic tiling of the 10-gon. Further argument shows that any other θ in the same chamber gives the same tiling

[1]Brief explanation: One first observes that the 2-dimensional faces of a 3-dimensional zonotope are translates of planar zonotopes spanned by subsets of the generating zones (see [21, p. 205]). These will all be parallelograms unless three of the lifted zones $\widetilde{v}_i, \widetilde{v}_j, \widetilde{v}_k$ are linearly dependent. A linear dependence relation among these lifts would be a multiple of z^τ, where $\tau = \{i,j,k\}$. This would imply $\theta \in H^\tau$, contradicting the choice of θ.

and that all rhombic tilings of the 10-gon arise in this way. An example of what might happen if the original zonotope were a hexagon and the lifted zonotope a 3-cube is shown in Figure 13; depending on its orientation in $\mathbb{R}^3$, the bottom of the cube would look like one of two tilings shown.

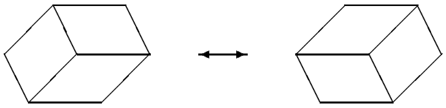

FIGURE 13. A flip of a 3-cube.

A move between adjacent chambers in the arrangement in Figure 12 corresponds to a simple local change in the corresponding tiling: for some embedded "3-cube" in the tiling, *flip* just that portion of the tiling as shown in Figure 13. So the chamber corresponding to a tiling is an i-gon if and only if the tiling has i embedded 3-cubes; for example the tiling on the left in Figure 11 corresponds to a triangular region, while that on the right corresponds to a pentagonal region.

We note that the situation described here is a piece of a very general theory of subdivisions [3, 1]. In particular, for any d-dimensional zonotope Z with n zones in $\mathbb{R}^d$, one can associate an arrangement of at most $\binom{n}{d+1}$ hyperplanes in $\mathbb{R}^{n-d}$ whose chambers correspond to certain tilings of Z. In our example it turns out to be *all* the rhombic tilings, but, in general, not all tilings can be obtained by the lifting procedure described above; see [3] for details. When $n = d + 3$ the derived arrangement will be 3-dimensional, and so theory of the present paper applies.

To conclude, let us apply the results of Section 1.3 to our walk on the tilings of a 10-gon. There are 40 vertices, 100 edges, and 62 regions, with $(p_3, p_4, p_5) = (50, 10, 2)$. The stationary probability of a tiling with i cubes is $(i-2)/76$. The eigenvalues and multiplicities (λ, m_λ) are $(1,1)$, $(\frac{1}{4}, 10)$, $(\frac{1}{20}, 30)$, and $(0, 21)$. After ℓ steps, the distance to stationarity satisfies

$$||K^\ell - \pi|| \leq 10 \left(\frac{1}{4}\right)^\ell .$$

5. A GEOMETRIC DESCRIPTION OF K

We return to the setting of Section 1, where $\mathcal{A}$ is a collection of n planes in $\mathbb{R}^3$ and K is the transition matrix of the walk on regions of the sphere (or, equivalently, on chambers). Recall that, in the notation of Section 1,

$$K(C, C') = \frac{1}{f_0} \Lambda(C, C'), \tag{6}$$

where $\Lambda(C, C')$ is the number of vertices v of C' such that $vC = C'$. Note that $\Lambda(C, C)$ is the number of vertices of C and that $\Lambda(C, -C) = 0$. The main result of this section is the following formula for $\Lambda(C, C')$ when $C' \neq \pm C$: If k is the number of sides of C' for which the sign vectors of C and C' agree (that is, the number of planes in the arrangement that do *not* separate C from C'), then

$$\Lambda(C, C') = k - 1.$$

This will be proved in Section 5.2 below (Lemma 2). We begin by describing the matrix Λ in terms of lunes.

5.1. **Lunes.** For a region D and a vertex v of D, let $\ell(v, D)$ be the *lune* determined by v and D as in Figure 14. Thus if H_1 and H_2 are the great circles bounding D and passing through v, and if H_i^+ is the hemisphere defined by H_i that contains D ($i = 1, 2$), then $\ell(v, D)$ is the intersection $H_1^+ \cap H_2^+$. Given two regions C, C', we define the *lunacy* of C with respect to C' to be the number of vertices v of C' such that $C \subseteq \ell(v, C')$.

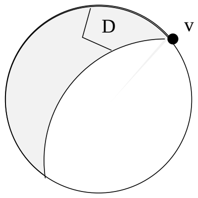

FIGURE 14. The lune $\ell(v, D)$

Proposition 3. *For any two regions C, C', $\Lambda(C, C')$ is equal to the lunacy of C with respect to C'.*

Proof. Assume, to simplify notation, that the sign vector of C' consists of all $+$'s. For a vertex v of C', we have $vC = C'$ if and only if the sign vector of vC is $+$ in the positions corresponding to the sides of C'. Now v has $+$ in all of these positions except two, where it has 0; so $vC = C'$ if and only if C already has $+$ in the two positions corresponding to the sides of C' that intersect at v. But this says precisely that $C \subseteq \ell(v, C')$. □

Understanding K, then, reduces to calculating lunacy. Figure 15 shows a simple example; here C is in the lune $\ell(v, C')$ but not the other two C'-lunes, so $\Lambda(C, C') = 1$. On the other hand, C' is in two of the four C-lunes, so $\Lambda(C', C) = 2$. Note the lack of symmetry.

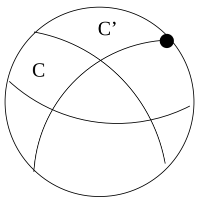

FIGURE 15. $\Lambda(C, C') = 1$.

There is a similar description of the transition matrix for the higher-dimensional hyperplane walks described in Section 3. One replaces the lunes by sets $\ell(F, C)$, where C is a chamber, F is a face of C, and $\ell(F, C)$ is an intersection of open half-spaces, one for each bounding hyperplane of C. What's special about the 3-dimensional case, however, is that lunacy is easy to compute. The computation depends on a simple geometric fact about polygons, related to "shellability".

5.2. **Shellability and the calculation of lunacy.** Consider a planar convex polygon P whose sides are extended to form lines $\ell_1, \dots, \ell_n$. If the polygon is viewed from any point x outside of it, one sees a contiguous set of its edges, and these are precisely the edges whose lines separate x from P. See Figure 16; here it is assumed that P is on the positive side of each ℓ_i, and the lines are labeled with $\pm$ to indicate which side x is on.

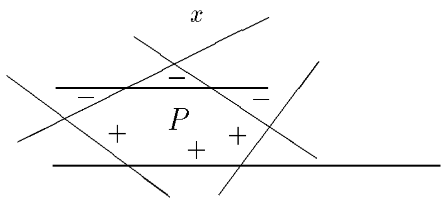

FIGURE 16. The sides visible from x.

All of this works equally well on the sphere:

Lemma 1 (Shelling lemma)**.** *Given a spherical polygon bounded, in cyclic order, by n great circles $\ell_1, \dots, \ell_n$, suppose that the interior of the polygon is on the positive side of each of these circles. Then any point on the sphere not on any of the circles is on the positive side of a cyclically contiguous subset of them.*

An analogue of the shelling lemma holds for convex polytopes in d-dimensional space [6] and for oriented matroids [17]. In the former case, contiguity is replaced by "shellability" of the set of visible faces, whence the name "shelling lemma". The latter case implies that everything we have done will work for arrangements of pseudocircles (cf. Section 2.4 above). See [21] and [4] for discussions of all of these topics. We omit the formal proof of the shelling lemma because it is treated thoroughly in the references cited and because, in the present low-dimensional case, it is quite believable from the picture.

Lemma 2 (Lunacy lemma)**.** *Given two regions C and C' that are neither equal nor opposite, we have*

$$\Lambda(C, C') = k - 1,$$

where k is the number of sides of C' for which the sign vectors of C and C' agree. Consequently,

$$\Lambda(C, C') + \Lambda(-C, C') = i - 2$$

if C' is an i-gon.

In Figure 15, for example, C' has 3 sides, one of which separates C from C'; so $k = 2$ and $\Lambda(C, C') = 1$, as we have already observed.

Proof of the lunacy lemma. Assume that C' has sign vector $++\cdots+$ and apply the shelling lemma to the polygon C', with x equal to any interior point of C. It follows that the sign pattern of C, restricted to the sides of C', will be a cyclic permutation of the string $++\cdots+--\cdots-$, where there are k $+$'s. Every pair of cyclically consecutive $+$'s corresponds to a lune of C' that contains C. Since there are $k-1$ such pairs, the lunacy $\Lambda(C, C')$ is indeed $k-1$. To prove the second assertion of the lemma, note that for each of the i sides of C' either C or $-C$ has the same sign as C'. Thus the k's for C and $-C$ sum to i. $\square$

Remark. If $C = C'$, then $\Lambda(C, C') = i$, while if $C = -C'$ then $\Lambda(C, C') = 0$. Hence $\Lambda(C, C') + \Lambda(-C, C') = i$ rather than $i - 2$ if $C = \pm C'$.

5.3. **Convergence rate examples.** Recall from Section 2.1 that the walk on regions is close to stationary after 2 steps for an arrangement of planes in $\mathbb{R}^3$ in general position. Now that we understand the matrix K, we can give examples where the walk is not close to stationary after 1 step. In other words, we want $\|K_C - \pi\|$ to be bounded away from 0 for an infinite family of general position arrangements with larger and larger n. The family of arrangements that we will use is a family $\mathcal{A}_n$ constructed by Füredi–Palásti [9], for which p_3, the number of triangles, is asymptotic to $2n^2/3$ as $n \to \infty$. (Recall from Section 2.1 that f_2, the total number of regions, is about n^2. So there are about $n^2/3$ non-triangular regions. Most of these are hexagons.) Fix a starting region C. We claim that for any triangular region C', either $\Lambda(C, C') = 0$ or $\Lambda(C, -C') = 0$. To see this, we may assume $C' \neq \pm C$. Then $\Lambda(C, C') + \Lambda(-C, C') = 1$ by the lunacy lemma, so one term is 0. Our claim now follows from the fact that $\Lambda(-C, C') = \Lambda(C, -C')$.

In view of the claim, there are $p_3/2$ triangular regions C' which cannot be reached from C in one step. Our main theorem, however, implies that this set $\mathcal{T}$ of triangles has stationary probability

$$\pi(\mathcal{T}) = \frac{p_3}{2} \cdot \frac{1}{2(f_0 - 2)}.$$

The definition (2) of total variation distance now implies that $\|K_C - \pi\| \geq \pi(\mathcal{T})$, which tends to $1/6$ as $n \to \infty$. Thus the walk for $\mathcal{A}_n$ is not close to stationary after one step.

Remark. On the other hand, there is a naturally occurring family of arrangements $\mathcal{B}_n$ for which the walk *is* close to random after one step. Here $\mathcal{B}_n$ is the *cyclic* arrangement, consisting of n great circles that form the sides of an n-gon in the Northern Hemisphere. There will, of course, also be an n-gon antipodal to this one in the Southern Hemisphere. $\mathcal{B}_n$ is a general position arrangement; for $n \geq 5$ there are $2n$ triangles and $n(n-3)$ quadrilaterals in addition to the two n-gons. The cases $n = 3, 4, 5, 6$ are shown in Figures 1, 2, 5, and 6 above. A straightforward but tedious calculation shows that, for any starting region C, $\|K_C - \pi\| \leq c/n$ for c a universal constant; thus the walk is close to random after one step when n is large.

6. Proof of Theorem 1

Recall that we are trying to calculate the stationary distribution π of the walk with transition matrix given by (6). The assertion is that

$$\pi(C) = \frac{i-2}{2(f_0 - 2)} \tag{7}$$

if C is an i-gon. There are two ways to proceed.

Method 1. As we remarked in the introduction, it suffices to show that the right-hand side of (7) is a probability distribution satisfying

$$\sum_C \pi(C) K(C, C') = \pi(C') \tag{8}$$

for all C'. Now we already know, by the Euler relation, that the right-hand side sums to 1 (cf. Section 2.2). So it suffices to show, for each C',

$$\sum_C (i(C)-2)K(C,C') = i(C')-2,$$

where $i(C)$ is the number of sides of C. Equivalently, we must show

$$\sum_C (i(C)-2)\Lambda(C,C') = f_0(i(C')-2). \tag{9}$$

Since $i(-C)=i(C)$, we can replace $\Lambda(C,C')$ on the left by the average

$$M(C,C') = \frac{\Lambda(C,C')+\Lambda(-C,C')}{2}$$

without changing the value of the sum. In view of the lunacy lemma, the left side of (9) becomes

$$\sum_C (i(C)-2)M(C,C') = \sum_C (i(C)-2)\frac{i(C')-2}{2} + 2(i(C')-2),$$

where the second term takes account of the fact that $M(\pm C', C') = i(C')/2$ instead of $(i(C')-2)/2$. Pulling out the factor $i(C')-2$, and recalling that $\sum_C (i(C)-2) = 2(f_0-2)$, we obtain (9). □

Method 2. We know that π exists and is characterized by (8), which can be rewritten

$$\sum_C \pi(C)\Lambda(C,C') = f_0\pi(C'). \tag{10}$$

Since $\Lambda(C,C') = \Lambda(-C,-C')$, it follows that $\pi(-C)=\pi(C)$. We may therefore rewrite (10) as

$$\sum_C \pi(C)M(C,C') = f_0\pi(C'),$$

with M as in the first proof. Using the lunacy lemma (and taking account of the terms in the sum where $C=\pm C'$), the equation becomes

$$\sum_C \pi(C)\frac{i(C')-2}{2} + 2\pi(C') = f_0\pi(C')$$

or, since $\sum_C \pi(C) = 1$,

$$\frac{i(C')-2}{2} + 2\pi(C') = f_0\pi(C').$$

Solving for $\pi(C')$, we obtain

$$\pi(C') = \frac{i(C')-2}{2(f_0-2)},$$

as required. □

This second proof is somewhat more satisfying than the first, since equation (7) appears naturally, rather than being pulled out of a hat. Note also that the second proof did not use the Euler relation; it therefore has the Euler relation as a consequence.

Remark. We are mystified by the factor $i-2$ in Theorem 1. To help appreciate the mystery (and Theorem 1) let us consider a different random walk on the chambers of a hyperplane arrangement, called the *local walk*. Suppose the walk is currently in region C bounded by i hyperplanes. Pick one of the bounding planes uniformly at random. The walk moves to the chamber adjacent to C along the chosen hyperplane. Call the transition matrix of this walk $H(C,C')$. If $i(C)$ denotes the number of sides of C, then

$$H(C,C') = \begin{cases} 1/i(C) & \text{if } C' \text{ is adjacent to } C \\ 0 & \text{otherwise.} \end{cases}$$

For this walk, an i-sided chamber C has stationary probability proportional to $i = i(C)$; moreover, this walk is reversible: $i(C)H(C,C') = i(C')H(C',C)$. The more vigorous walk $K(C,C')$ that we have been studying is not reversible except in special cases. It is one of only a few families of nonreversible walks where the stationary distribution is known explicitly. For the braid arrangement of Section 4.1, the local walk corresponds to mixing a deck of cards by adjacent transpositions, whereas the walk of this paper corresponds to the (much faster) riffle shuffling. For tilings (cf. Section 4.2), physicists currently use the local walk (cube flips) for simulating a random tiling. We hope that the walk described here will offer vast speed-ups.

7. Final remarks

The plane arrangements $\mathcal{A}$ in $\mathbb{R}^3$ that we have been considering in this paper occur in the literature under the name *line arrangements*. In fact, a plane through the origin in $\mathbb{R}^3$ is the same as a line in the projective plane P^2, so we can think of $\mathcal{A}$ as an arrangement of lines in the plane. Recall that the points of P^2 are the lines through the origin in $\mathbb{R}^3$. Since a line through the origin in $\mathbb{R}^3$ corresponds to a pair of antipodal points on the sphere S^2, we get a 2-to-1 map $S^2 \to P^2$. The great circles in our spherical pictures are the inverse images of the lines in P^2 under this map. As a practical matter, if P^2 is viewed as the affine plane with an extra line at infinity, one goes from the projective picture to the spherical picture by drawing the projective picture on the Northern Hemisphere, the line at infinity becoming the equator.

For a simple example, consider the arrangement of four lines in P^2 consisting of the three lines shown in Figure 17 together with the line at infinity. The corresponding spherical picture is Figure 2 in the introduction. A more complicated example of a projective picture was given in Figure 7 of Section 2.3. The cell-decomposition of S^2 that we have been using in this paper is obtained by lifting an analogous cell-decomposition of P^2. Thus there is a pair of antipodal cells in S^2 for each cell in P^2.

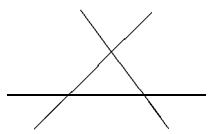

FIGURE 17. Four lines in P^2; the line at infinity is included.

There is an extensive literature on line arrangements (and "pseudoline" arrangements) going back to the 1820's. Much is known, but there are still many open questions. See [13, 10] for surveys. Some of the more interesting results and open questions concern the polygon counts p_i $(i \geq 3)$ where, following standard conventions, we now denote by p_i the number of i-gons in the cell decomposition of P^2; this is half of what was called p_i in Section 2. A sample result is that for an arrangement in general position, one has

$$p_3 = 4 + \sum_{i \geq 5} (i-4) p_i. \tag{11}$$

(The reader can check that this equation holds for each column of Table 1 in Section 2.1, after the numbers in that table are cut in half.) Moreover, given any sequence $p_3, p_5, p_6, p_7, \ldots$ of natural numbers satisfying (11), one can always find a general position arrangement with those polygon counts. One has no control over p_4, however, and, indeed, very little is known about p_4. Equivalently, one has no control over the number of lines in the arrangement. Thus we are still very far from knowing, for a given n, what vectors $(p_3, p_4, \ldots, p_n)$ can occur.

See [13, 10] for a wealth of further results, conjectures, and open questions.

References

[1] Margaret M. Bayer and Keith A. Brandt, *Discriminantal arrangements, fiber polytopes and formality*, J. Algebraic Combin. **6** (1997), no. 3, 229–246.

[2] T. Patrick Bidigare, Phil Hanlon, and Daniel N. Rockmore, *A combinatorial description of the spectrum for the Tsetlin library and its generalization to hyperplane arrangements*, Duke Math. J., to appear.

[3] Louis J. Billera and Bernd Sturmfels, *Fiber polytopes*, Ann. of Math. (2) **135** (1992), no. 3, 527–549.

[4] Anders Björner, Michel Las Vergnas, Bernd Sturmfels, Neil White, and Günter M. Ziegler, *Oriented matroids*, Encyclopedia of Mathematics and its Applications, vol. 46, Cambridge University Press, Cambridge, 1993.

[5] Kenneth S. Brown and Persi Diaconis, *Random walks and hyperplane arrangements*, Ann. Probab., to appear.

[6] H. Bruggesser and P. Mani, *Shellable decompositions of cells and spheres*, Math. Scand. **29** (1971), 197–205 (1972).

[7] Veit Elser, *Random tiling structure of icosahedral quasicrystals*, Philosophical Magazine B **73** (1996), 641–656.

[8] James Allen Fill, *An exact formula for the move-to-front rule for self-organizing lists*, J. Theoret. Probab. **9** (1996), no. 1, 113–160.

[9] Z. Füredi and I. Palásti, *Arrangements of lines with a large number of triangles*, Proc. Amer. Math. Soc. **92** (1984), no. 4, 561–566.

[10] Jacob E. Goodman, *Pseudoline arrangements*, Handbook of discrete and computational geometry (J. E. Goodman and J. O'Rourke, eds.), CRC Press, Boca Raton, 1997, pp. 83–109.

[11] Branko Grünbaum, *Convex polytopes*, Pure and Applied Mathematics, vol. 16, Wiley-Interscience, New York, 1967, with the cooperation of Victor Klee, M. A. Perles and G. C. Shephard.

[12] ———, *Arrangements of hyperplanes*, Proceedings of the Second Louisiana Conference on Combinatorics, Graph Theory and Computing (Louisiana State University, Baton Rouge, La., March 8–11, 1971) (R. C. Mullin, K. B. Reid, D. P. Roselle, and R. S. D. Thomas, eds.), Louisiana State University, 1971, pp. 41–106.

[13] ———, *Arrangements and spreads*, CBMS Regional Conference Series in Mathematics, vol. 10, American Mathematical Society, Providence, R.I., 1972.

[14] Branko Grünbaum and G. C. Shephard, *Simplicial arrangements in projective 3-space*, Mitt. Math. Sem. Giessen (1984), no. 166, 49–101.

[15] Christopher L. Henley, *Random tiling models*, Quasicrystals: the state of the art (D. P. DiVincenzo and P. J. Steinhardt, eds.), Directions in Condensed Matter Physics, vol. 11, World Scientific Publishing Co. Inc., River Edge, NJ, 1991, pp. 429–524.
[16] John G. Kemeny and J. Laurie Snell, *Finite Markov chains*, The University Series in Undergraduate Mathematics, D. Van Nostrand Co., Inc., Princeton, N.J.-Toronto-London-New York, 1960.
[17] Arnaldo Mandel, *Topology of oriented matroids*, Ph.D. thesis, University of Waterloo, 1982.
[18] Peter Orlik, *Introduction to arrangements*, CBMS Regional Conference Series in Mathematics, vol. 72, American Mathematical Society, Providence, R.I., 1989.
[19] Peter Orlik and Hiroaki Terao, *Arrangements of hyperplanes*, Grundlehren der Mathematischen Wissenschaften, vol. 300, Springer-Verlag, Berlin, 1992.
[20] Richard P. Stanley, *Enumerative combinatorics. Vol. 1*, Cambridge Studies in Advanced Mathematics, vol. 49, Cambridge University Press, Cambridge, 1997, with a foreword by Gian-Carlo Rota, corrected reprint of the 1986 original.
[21] Günter M. Ziegler, *Lectures on polytopes*, Graduate Texts in Mathematics, vol. 152, Springer-Verlag, New York, 1995.

Cornell University, Ithaca, NY 14853-7901